Mean field model of Actin Cortex polymerization - depolymerization dynamics

Senior Year Physics Project

By: Nadav Porat
Advisor: Prof. Arik Yochelis

August 30, 2023

Contents

1 Introduction

1.1 Biology Background

1.1.1 The Actin Cortex

Most animal cells, contrary to plant cells, lack a cell wall. The absence of a rigid cell wall allows animal cells to continuously change their shape based on their surroundings and functions. However, the animal cell's membrane is thin-skinned, so it is not sufficient to protect and sustain the cell in its dynamic environment (e.g., withstanding pressures of $10^2 - 10^3$ Pa [3]). Animal cells derive their required stiffness from a network of proteins from the actin family called the *actin cortex*. The actin cortex is positioned on the inner side of the membrane, supporting its structure and contributing to the cell's movement. The actin cortex is depicted in red in Figure 1.

The actin network is dense, providing strength to the cell's membrane against its environment. However, the actin cortex is more than just a structure for stiffening the cell's membrane. The cortex is a dynamic environment, with its proteins constantly undergoing turnover (replacement of old proteins with new ones). This turnover causes the actin cortex to behave like a viscous fluid. When subjected to local stress, it can use actin turnover and the dissociation of crosslink proteins to reshape itself and adapt to the local disturbance [4]. Due to this property, actin networks are often referred to as "active gels".

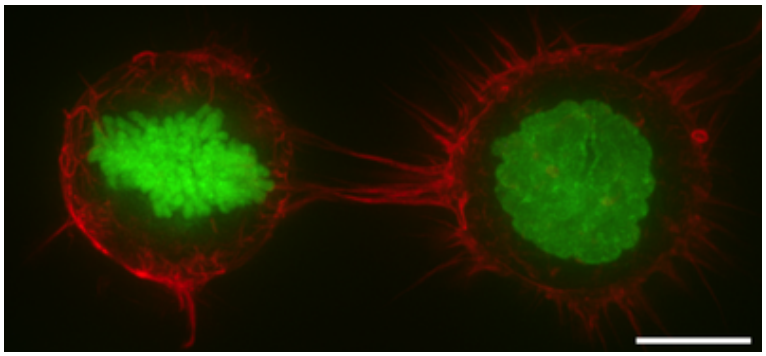

Figure 1. *Human HeLa cells stained with various chemicals. F-actin in red, chromosomes in green. Scale bar: 10 micrometers. Taken from Wikipedia.*

1.1.2 Actin Polymerization and Depolymerization

Actin filaments (F-actin) are long, thin, flexible fibers polymerized from actin monomers (G-actin). Filaments assemble at one end (the "leading edge," "new end," or "+end") and disassemble at the other end, as shown in Figure 2. These filaments are approximately 7 nm in diameter and can be several micrometers long [2]. Actin monomers also bind to ATP, which accelerates polymerization. When G-actin becomes "old," its ATP hydrolyzes into ADP. Actin filaments collectively form actin networks such as stress fibers, filopodia, lamellipodia, and the cell/actin cortex.

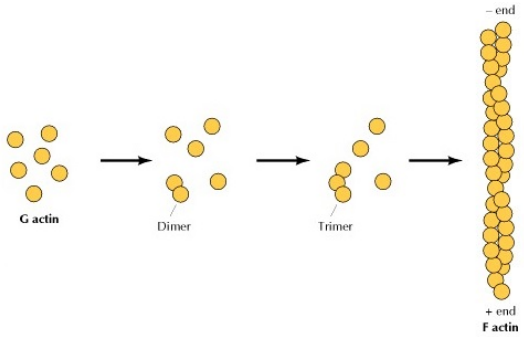

Figure 2. *Actin monomers (G-actin) polymerize to form actin filaments (F-actin). The process starts with the formation of dimers and trimers, which then grow by adding monomers to both ends. From [2].*

In addition to actin proteins, various actin-binding proteins are required to form and maintain actin networks. Some of these proteins function as crosslinkers, ARP2/3, and Cofilin. ARP2/3 and Cofilin are especially significant to us as they regulate the polymerization and depolymerization of actin filaments.

The initial step of actin filament assembly (nucleation) involves the formation of a small aggregate of actin monomers, which then elongates at the new end. Actin nucleation can occur through various mechanisms, one of which involves the ARP2/3 complex. This complex provides a nucleation core that binds to actin monomers, initiating the polymerization of actin filaments (Figure 3B). The ARP2/3 complex also contributes to actin branching, which will be discussed later.

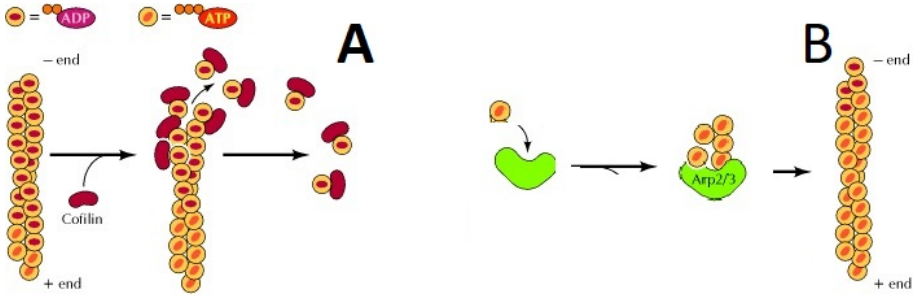

Figure 3. *Actin polymerization and depolymerization with ARP2/3 and Cofilin. (A) Actin polymer disassembly from the "old" end with Cofilin. (B) Actin polymer formation from an ARP2/3 nucleation site. Modified from [2].*

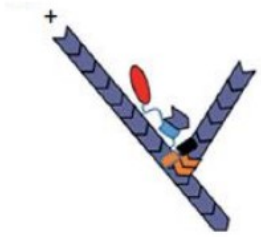

Figure 4. *ARP2/3 (orange) induces branching of F-actin (blue). In red is a protein called WASP that aids ARP2/3 in the branching process. Taken from [1].*

The key protein regulating actin filament disassembly is Cofilin. It binds to actin filaments and accelerates the dissociation of actin monomers. Cofilin binds more effectively to ADP-actin, making the old end of the actin filament more susceptible to disassembly (Figure 3A).

When G-actin is added to F-actin, it doesn't necessarily lengthen the F-actin strand. Instead, with the assistance of ARP2/3, it can initiate a new branch of F-actin at an angle from the original F-actin strand, as depicted in Figure 4. Branching involves two monomers, as opposed to the single monomer used in elongation. This daughter branch is estimated to be at an angle of about 78° from the parent branch [10]. This branching mechanism results in a complex interwoven network of strong F-actin strands with varying angles and connections to each other.

1.2 Project Objective: Simulating Actin Cortex Dynamics

Recently, Prof. Bernheim's group conducted experiments that grow an actin cortex under well defined conditions [1]. The group managed to recreate the turnover effect of the polymers by combining the appropriate proteins in a controlled environment (outside of a cell), and measure it as well. Figure 5 displays a relevant result from their experiments. The figure shows the evolution of an actin network over time. Notably, the density distribution of actin initially starts symmetrically, then becomes bimodal, and finally non-symmetric. This dynamic appears as if a portion of the actin gel is severed and then depolymerized.

The constant turnover of actin, involvement of numerous proteins, and the small size of actin molecules make studying and modeling actin networks challenging, not to mention simulating it. Mathematical models of actin networks exist in the literature [8] [9], but we did not find a model that describes the the group's results. For the purpose of modelling the Bernheim's empirical results, Prof. Yochelis and his colleagues formulated a set of equations that describe the growth of an actin network in a controlled environment. The model, to be presented in later sections, comprises a set of nonlinear PDEs involving both temporal and spatial aspects. The model aims to account for the intricate dynamics of monomer polymerization and protein-induced depolymerization.

In this project, we focus on testing and validating the model. We use numerical techniques to analyze the model's behaviour under different boundary conditions, and use the results to refine the equations. The ultimate goal of the project is to simulate qualitatively the physical and biological phenomenon measured in Bernheim's group experiments.

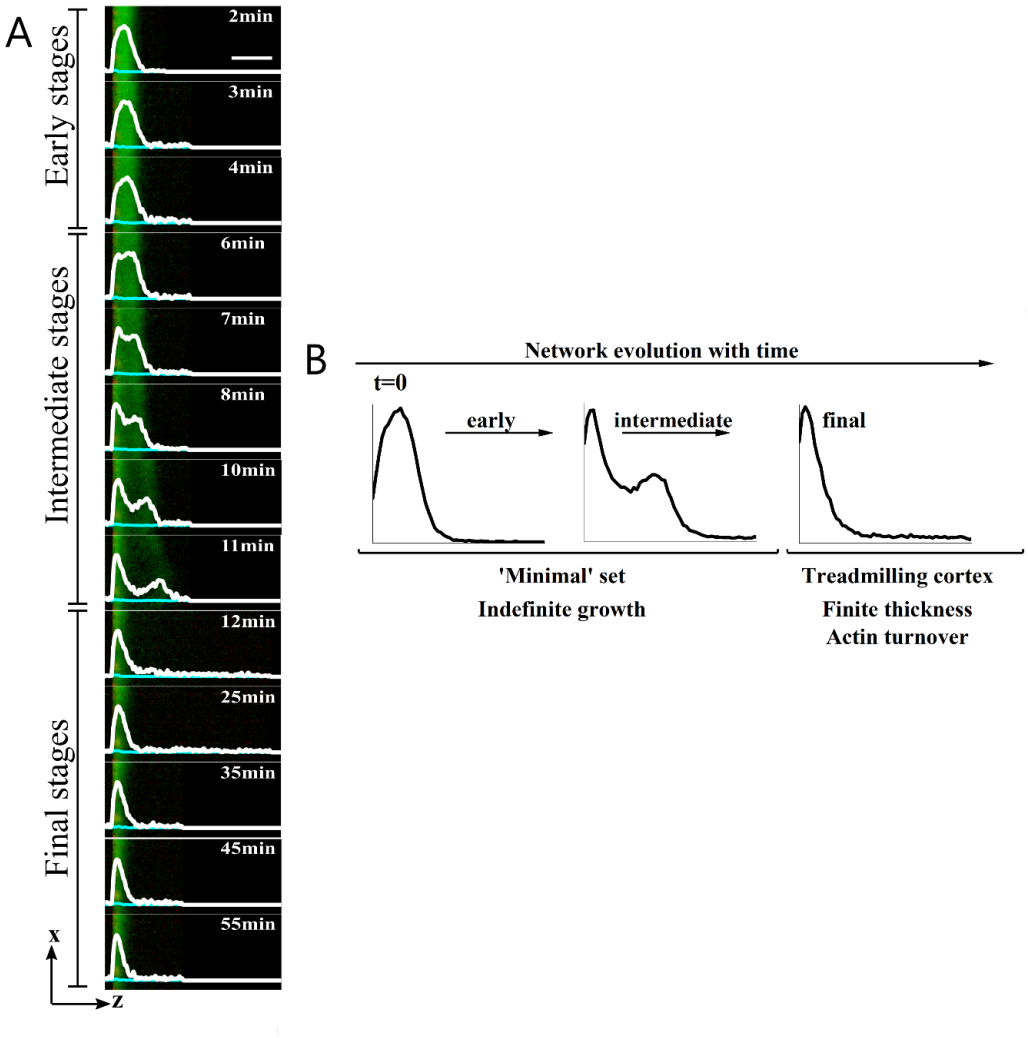

Figure 5. *Growth dynamics of the Actin-Cofilin system. (A) Actin gel (green) polymerizing at different time points. Measured intensity profiles are shown in white. Scale bar: 10 micrometers. (B) Schematic actin density profiles at different stages of evolution. Modified from [1].*

2 Model Equations

2.1 Bulk equations

The model, proposed by Prof. Yochelis, Prof. Bernheim, and Prof. Gov, was constructed based on [1]. The equations are formulated for the 3D case, with the z axis representing the actin growth axis. The analysis in the next chapter was performed on a 1D model derived from this one. Figure 6 shows a 3D representation of an actin cortex that can be used as a reference for this model, taken from Bernheims's group. The equations for the bulk are as follows:

$$\frac{\partial p}{\partial t} = -v\partial_z p - \alpha c_b p \tag{1a}$$

$$\frac{\partial m}{\partial t} = \nabla \cdot (D_m(1-\beta p)\nabla m) + \alpha c_b p \tag{1b}$$

$$\frac{\partial c_f}{\partial t} = D_c \nabla^2 c_f - k_s c_f p + \alpha c_b p \tag{1c}$$

$$\frac{\partial c_b}{\partial t} = -v\partial_z c_b + k_s c_f p - \alpha c_b p \tag{1d}$$

Where:

$$v = a_{br}k_{br}m^2\Big|_{z=0} + a_{gr}k_{gr}(m-m_c)\Big|_{z=0} \tag{2}$$

In this model, p, m, c_f, c_b represent the concentrations of F-actin, G-actin, free Cofilin, and bound Cofilin as functions of 3D space and time. The flux and conversions between species in the equations are based of regular methods that can be found in appendix 5.1. A comprehensive description of the parameters is provided in Table 1.

The key concepts in this model include:

- The term $\alpha c_b p$ accounts for the depolymerization of F-actin by bound Cofilin. The parameter α can be a constant, or a function that varies according to the polymer age.
- The term $k_s c_f p$ accounts for the binding of free Cofilin to F-actin.

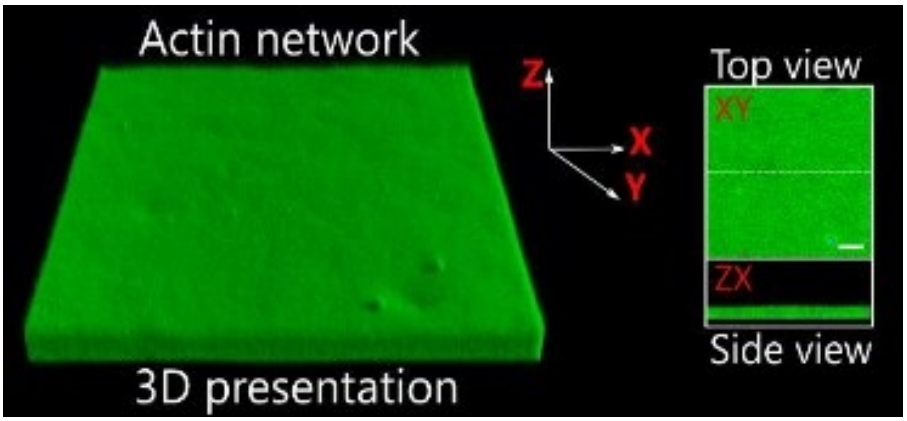

Figure 6. *Laser scanning images of a cortical actin gel: (left) 3D presentation and (right) top-view image is the sum of intensities along the z-axis, and side-view measured along the white line in top-view. Scale bar is 5 micrometers. Modified from [1].*

- Both m and c_f diffuse, but the diffusion of the monomers is slowed down locally by the presence of a dense actin network p.
- F-actin is propelled forward by polymerization that is happening only at the boundary $z = 0$ which is the plus end of the polymer, thus its propagation speed v is calculated at the boundary.
- The two terms in v describe the two ways monomers are added to an existing polymer, either by branching or growing (subsection 1.1.2).
- Growing isn't initiated until a critical concentration of monomers m_c at the boundary is reached.
- The monomer flux is polymerized at $z = 0$ and its accounted for in the boundary conditions (described below).

2.2 Boundary conditions

The boundary conditions at $z = 0$ are extremely important, because they determine the polymerization in the system. The boundary conditions are:

$$\nabla p = 0 \tag{3a}$$

$$\sum J_{total} = J_m + J_p = D_m(1 - \beta p)\nabla m - vp = 0 \tag{3b}$$

$$\nabla c_f = 0 \tag{3c}$$

$$c_b = 0 \tag{3d}$$

The boundaries at $z = L$:

$$p = 0 \tag{4a}$$

$$\nabla m = 0 \tag{4b}$$

$$\nabla c_f = 0 \tag{4c}$$

$$c_b = 0 \tag{4d}$$

The rest of the boundaries at x and y are simple no-flux boundaries. In equation (3b) we equated the boundary m flux with the negative p flux. The reasoning is that the m flux that is coming from the positive z (bulk of the system), polymerizes at the boundary $z = 0$ and becomes p.

The addition of polymers to the system is essentially described by the p flux in equation (1a.) The transition $m \to p$ though is described in boundary (3b). So a part of the conversion is treated in the boundary and the other part in the bulk, with v linking between them. This fact made the boundary conditions for the polymerization extremely complex. Many times throughout the project, we changed and refined the boundary conditions, guided by intuition, numerical performance, and physical or biological laws.

2.3 Nondimensionalization of Equations

The model in subsections 2.1 - 2.2 was developed with dimensions according to Table 1. However, since we are primarily interested in reproducing biological phenomena, a dimensionless model proves to be more useful. We utilized the method of repeating variables, introduced in [7], to reduce the dimensions of the model. The repeating variables we selected for reducing other variables are a_{gr}, D_m, and m_c. We chose them because they are independent, remain constant throughout the model, and encompass all of the model's dimensions.

The following reduction was employed:

$$\begin{aligned}
&(\tilde{p}, \tilde{m}, \tilde{c_f}, \tilde{c_b}) = \frac{(p, m, c_f, c_b)}{m_c}, (\tilde{k_s}, \tilde{k_{gr}}, \tilde{\alpha}) = m_c a_{gr}^2 \frac{(k_s, k_{gr}, \alpha)}{D_m} \\
&\tilde{D_c} = \frac{D_c}{D_m}, \tilde{k_{br}} = a_{gr}^2 m_c^2 \frac{k_{br}}{D_m} \\
&\tilde{\beta} = \beta m_c, \tilde{x} = \frac{x}{a_{gr}}, \tilde{t} = D_m \frac{t}{a_{gr}^2}
\end{aligned} \tag{5}$$

Substituting the reduced parameters into the model and removing the tildes results in nearly identical equations. Specifically, only equations (1b), (2), and (3b) are affected, and they are replaced by:

$$\frac{\partial m}{\partial t} = \nabla \cdot ((1 - \beta p)\nabla m) + \alpha c_b p \tag{6}$$

$$v = a_{br} k_{br} m^2 \big|_{z=0} + k_{gr}(m-1)|_{z=0} \tag{7}$$

$$\sum J_{total} = J_m + J_p = (1 - \beta p)\nabla m - vp = 0 \tag{8}$$

The dimensional model wasn't extensively utilized during the project, as most of the results were obtained using the dimensional model.

2.4 Parameters and variables

Symbol	Units	Dimensions	Value	Description
p	μM	NL^{-3}	$p(x,y,t)$	Actin polymer density
m	μM	NL^{-3}	$m(x,y,t)$	Actin monomer density
c_f	μM	NL^{-3}	$c_f(x,y,t)$	Free Cofilin density
c_b	μM	NL^{-3}	$c_b(x,y,t)$	Bound Cofilin density
v	$\frac{\mu m}{s}$	Lt^{-1}	$v_p(x,y,t)$	Protein polymerization velocity.
a_{br}	μm	L	0.003	Length contribution of one monomer due to growing.
a_{gr}	μm	L	$sin(78°)a_{br}$	Length contribution of one monomer due to branching.
k_{br}	$\frac{1}{s\cdot(\mu M)^2}$	$L^6N^{-2}t^{-1}$	$2.16 \cdot 10^{-5}$	Rate of actin polymerization to branching. From [6] k_{br}^{side} multiplied by $40nM$ ARP2/3 concentration from [1]
k_{gr}	$\frac{1}{s\cdot\mu M}$	$L^3N^{-1}t^{-1}$	8.7	Rate of actin polymerization to elongation, from [6]
k_s	$\frac{1}{s\cdot\mu M}$	$L^3N^{-1}t^{-1}$	2 (?)	Rate of severing proteins on polymerized actin (?). This rate is not exactly known.
D_m	$\frac{(\mu m)^2}{s}$	L^2t^{-1}	8.4	Diffusion of actin monomers in solution. From [1]
D_c	$\frac{(\mu m)^2}{s}$	L^2t^{-1}	10	Diffusion of free Cofilin in solution. From [5].
β	$\frac{1}{\mu M}$	$N^{-1}L^3$	0.1 (?)	$\frac{1}{p_{max}}$ where p_{max} is the maximum density of actin gel. At p_{max} the gel is too dense for the monomers to diffuse.
α	$\frac{1}{s\cdot\mu M}$	$L^3N^{-1}t^{-1}$	0.2 (?)	Effective severing rate. May be a function or a constant.

Table 1. *Parameter values*

3 Analysis

3.1 Bulk analysis - periodic model

In this section, we delve into the dynamics of the bulk in our actin cortex model. The investigation involves discretizing the bulk equations, employing periodic boundary conditions, and implementing the process using Python.

Notice that from this section forward we tread the 1D model, in which x is the axis of actin growth:

$$z \to x$$

The full 1D version of the model is described in appendix 5.3.

To begin, we discretized the model introduced in the section 2.1. For equations (1a) and (1d), we used a backward finite difference scheme. For equations (1b) through (1c), we opted for a central finite difference scheme. This choice was driven by the behavior of equations for p and c_b, resembling a positive traveling wave. This discretization strategy proved effective for these variables. The discretization of the m equation followed the approach outlined in appendix 5.2. Here's the discretization of the bulk equations:

$$p_i^{n+1} = p_i - \frac{\Delta t}{\Delta x} \cdot v(p_i - p_{i-1}) - Depoly \tag{9a}$$

$$\begin{aligned} m_i^{n+1} = m_i + D_m \frac{\Delta t}{2\Delta x^2} \big[&(2 - \beta(p_i + p_{i+1}))(m_{i+1} - m_i) \\ &- (2 - \beta(p_i + p_{i-1}))(m_i - m_{i-1}) \big] + Depoly \end{aligned} \tag{9b}$$

$$c_{f,i}^{n+1} = c_{f,i} + D_c \frac{\Delta t}{\Delta x^2}(c_{f,i+1} + c_{f,i-1} - 2c_{f,i}) - Bind + Depoly \tag{9c}$$

$$c_{b,i}^{n+1} = c_{b,i} - v\frac{\Delta t}{\Delta x}(c_{b,i} - c_{b,i-1}) + Bind - Depoly \tag{9d}$$

Where:

$$Depoly = \Delta t\, \alpha c_{b,i} p_i \tag{10}$$

$$Bind = \Delta t\, k_s c_{f,i} p_i \tag{11}$$

To account for the absence of boundaries, the periodic conditions were applied:

$$p(x + L) = p(x), \quad m(x + L) = m(x) \tag{12a}$$

$$c_f(x + L) = c_f(x), \quad c_b(x + L) = c_b(x) \tag{12b}$$

In the absence of boundaries, v was replaced by a positive constant:

$$v = \text{const} \tag{13}$$

Figure 8 presents the outcomes. The graph depicts the initial state with polymers near the edge, followed by their migration to the right. In particular, figure A highlights the binding of free Cofilin with actin polymers (so that free Cofilin became bound Cofilin). Additionally, an increase in monomer concentration is evident due to the depolymerization caused by bound Cofilin. Part B of the figure illustrates the shift of the actin "wave" from the end of the domain

to its beginning. The simultaneous movement of bound Cofilin and polymers can be observed, alongside a decrease in polymer concentration in favor of monomers. Moreover, monomer diffusion is observed. The assessment also verified mass conservation - Figure 7 displays the deviation of the total monomer/Cofilin concentration from its initial value. Remarkably, the deviation's magnitude is 10^{-13}, likely due to numerical imprecision.

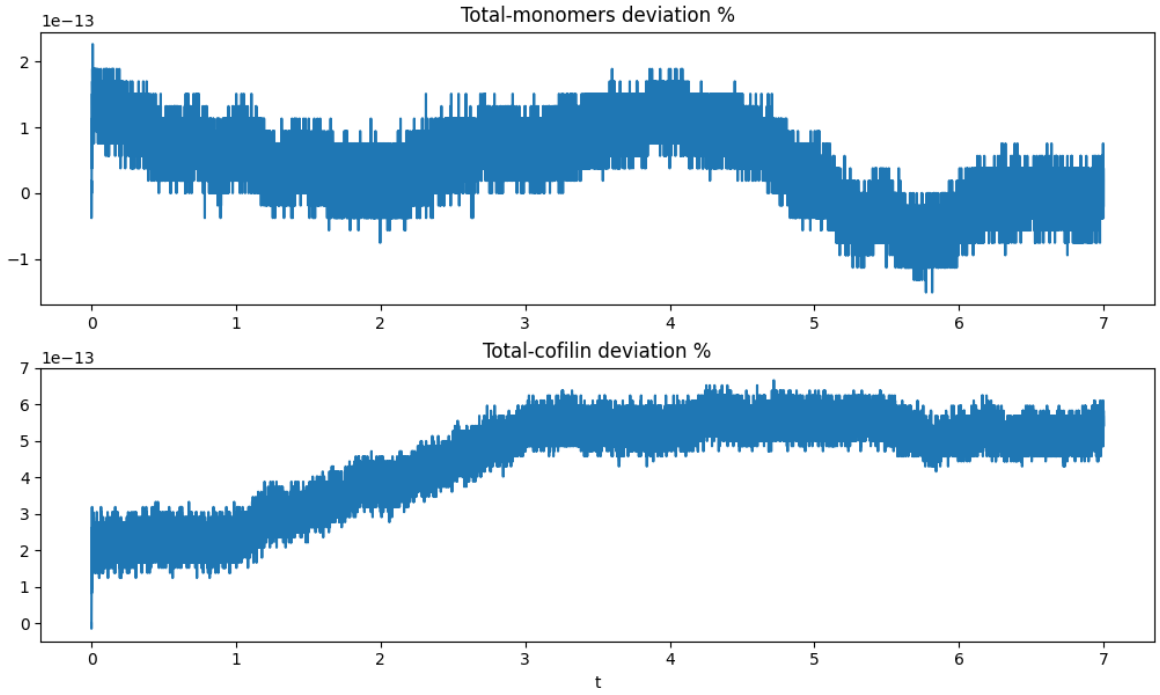

Figure 7. *Deviation of the total monomer/Cofilin concentration from its initial value for Figure 8. Each point represents the spatial integral of monomers/Cofilin at time point t, expressed as a percentage deviation from the corresponding integral value at $t = 0$.*

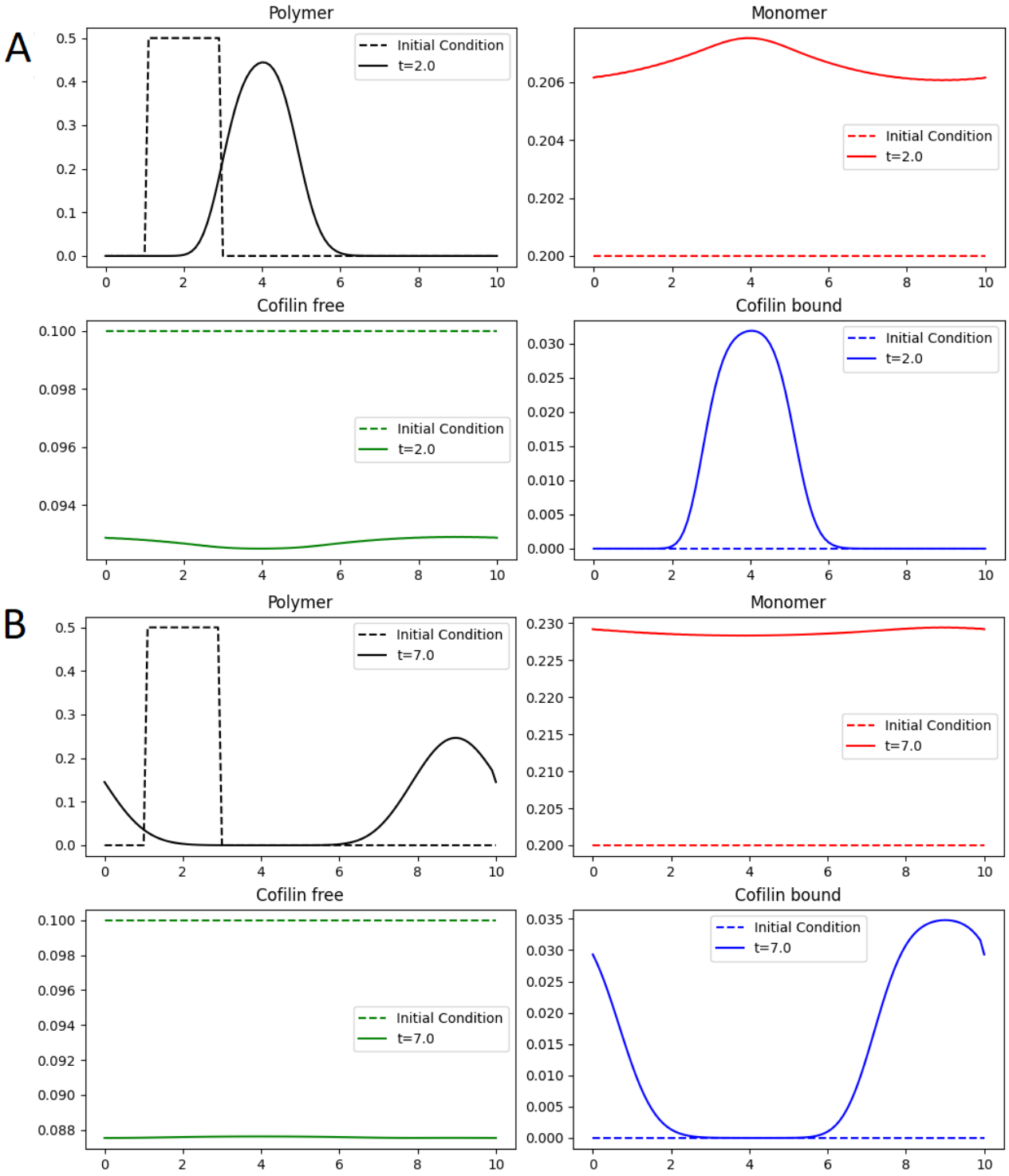

Figure 8. *Numerical results for the simplified periodic model. The y-axis represents concentration, and the x-axis represents space. The dashed lines depict the initial condition, while the solid lines show the solution at a certain time. Panel A presents the solution at $t = 2s$, displaying a traveling wave. Panel B illustrates the solution at $t = 7s$.*

3.2 Full model analysis

Moving forward, we address the complete model introduced in subsections 2.1 - 2.2. Again, the model is in 1D and the full 1D equations are presented in appendix 5.3. The objective is to discretize and implement this model using Python. We employed the bulk discretization method outlined in subsection 3.1, but with boundaries that define a closed box with polymerization at the left end.

For the inclusion of polymerization, the variable v is defined as:

$$v = a_{br}k_{br}m_0^2 + a_{gr}k_{gr}(m_0 - m_c) \tag{14}$$

The discretization of the right boundary is as follows:

$$p_M = 0 \tag{15a}$$
$$m_M = m_{M-2} \tag{15b}$$
$$c_{f,M} = c_{f,M-2} \tag{15c}$$
$$c_{b,M} = 0 \tag{15d}$$

Discretization of the left boundary:

$$p_0 = p_1 \tag{16a}$$
$$c_{f,0} = c_{f,2} \tag{16b}$$
$$c_{b,0} = 0 \tag{16c}$$

The discretization of m's left boundary is addressed in detail (following appendix 5.2:

$$\begin{aligned}\sum J_{total} = J_m + J_p = D_m(1-\beta p)\frac{\partial m}{\partial x} - vp = 0 \\ \Rightarrow 0 = D_m(1-\beta p_0)\frac{m_{-1} - m_1}{2\Delta x} - p_0 v \\ \Rightarrow m_{-1} = m_1 - \frac{2\Delta x}{D_m(1-\beta p_0)}p_0 v\end{aligned}$$

Notice that v is determined by m_0^n. Setting $i = 0$ in (9b), substituting m_{-1}, and canceling *Depoly* (no depolymerization on the boundary, $c_b = 0$), results in:

$$m_0^{n+1} = m_0 + D_m\frac{\Delta t}{2\Delta x^2}\left[(2-\beta(p_0+p_1))(m_1-m_0) - (2-\beta(p_0+p_{-1}))(m_0-m_{-1})\right] \tag{17}$$

With $p_{-1} = p_0$.

The simulation results are presented in Figure 10. The figure shows the initial state, where polymers are concentrated at the left edge, along with monomers and free Cofilin. In Figure 10A, polymerization occurs at $x = 0$, converting monomers to polymers and propelling existing polymers to the right. Binding of Cofilin and depolymerization are also evident. In Figure 10B, further polymerization takes place, while Cofilin-driven depolymerization leads to lower polymer concentration. Interestingly, in this simulation, α and k_s are spatially constant.

In Figure 9, the deviation for this simulation is shown. It is notably larger than before. Specifically, the simulation's progression reveals a significant increase in the total quantity of monomers, while the total amount of Cofilin decreases. By $t = 10s$, monomers decrease by 0.8%, and Cofilin increases by 0.7%. It is evident that the non-conservation of matter in this context is a significant issue that requires thorough investigation. Further discussion of this issue is given in subsection 4.1.

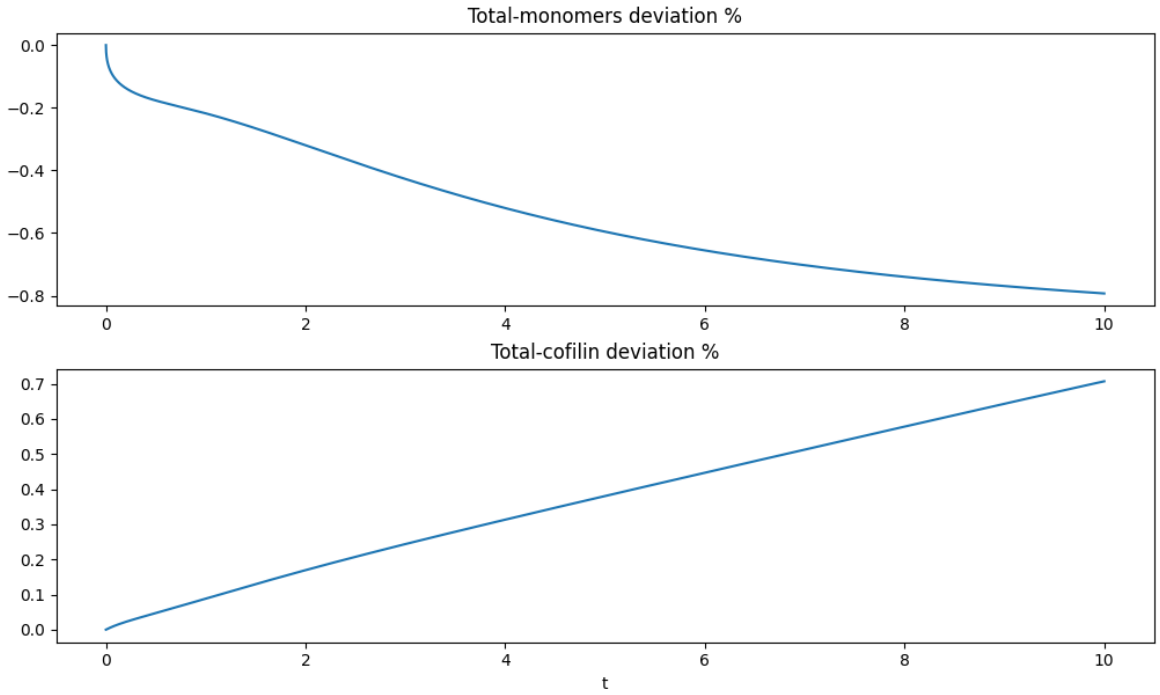

Figure 9. *Deviation of the total monomer/Cofilin concentration from its initial value for Figure 10. Each point represents the spatial integral of monomers/Cofilin at time point t, expressed as a percentage deviation from the corresponding integral value at $t = 0$.*

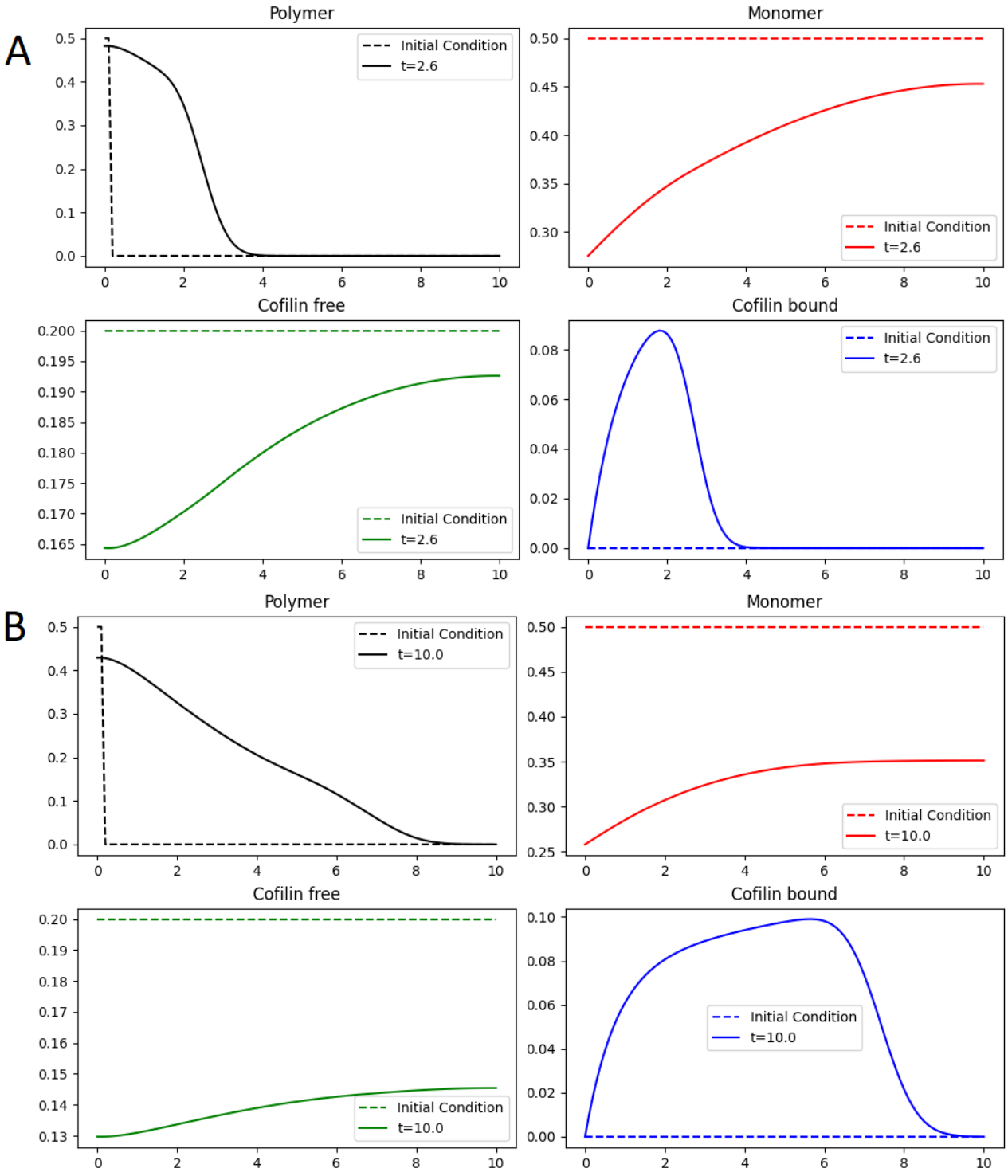

Figure 10. *Solution results for the full model at two time steps: Panel A - $t = 2.6s$, Panel B - $t = 10s$.*

4 Conclusions and discussion

4.1 Conclusions

The bulk analysis 3.1 of the model yielded results that we expected. Among these consistent behaviours are:

- Conversion of free Cofilin to bound Cofilin in areas with polymers.
- Homogeneous diffusion of c_f and non-homogeneous diffusion of m.
- Movement of p and c_b through the medium.
- Conservation of matter.

The full analysis 3.2 also reproduced some behaviours of the biological system that we aimed to model, namely:

- Polymerization speed v that is dependent on boundary monomer concentration.
- Critical monomer value m_c that limits the polymer's growth.
- Severing of a "chunk" of polymers.

With that being said, the model is still incomplete, it has flaws, and biological behaviours that we didn't manage to reproduce. On these, we will dive in further detail:

Matter conservation in the full model
As mentioned in the 3.2 section, the simulation of this section does not conserve matter. Throughout the project, these results posed significant challenges. The adequacy of the bulk equations has been established through the outcomes in the 3.1, so we can deduce that the boundary conditions lead to deviations in the system's mass quantity. The discrepancy in matter conservation raises questions about the validity of our boundary conditions. This could indicate that the specified boundary conditions, intended to describe the polymerization process, are inaccurately formulated. Alternatively, the boundary conditions might be accurately formulated, but issues could arise in the discretization process or its code implementation, potentially leading to artificial flux. Moreover, it is possible that both the boundary conditions and discretization are correctly established, but our interpretation of the boundary conditions for a closed system is incorrect.

Aging mechanism
The model overlooks certain factors present in biological realities, notably the absence of a proper aging mechanism. An attempt was made to incorporate this mechanism by introducing a spatially varying depolymerization factor, $\alpha = \alpha(x)$. This approach is rooted in the rationale that older proteins typically occupy more distant regions within the system due to their larger x values. The results were not shown here due to lack of significance. I believe that this implementation overly simplifies the mechanism, and an alternative approach that tracks the age of polymers would likely yield more accurate outcomes.

4.2 Personal experience

In the course of this project, I encountered the process of modeling a biological system for the first time. Early on, my advisor told me about the complexity of modeling biological systems due to the absence of governing conservation laws, as there are in physics. As I continued with the process of modeling and conducting numerical testing, the strength of this statement became apparent. The absence of a rigid, overarching law to derive equations from introduced difficulties to this project.

The mathematical modeling process was full of uncertainties that required that I study certain new methods and techniques. For example, I had to study numerical methods I was unfamiliar with, such as discretization of non-homogeneous diffusion, and the use of ghost points for nontrivial boundary conditions. Additionally, I had to study the biology of actin, and the different proteins that interact with it. I was also intrigued by the use of chemistry's mass action law for biological processes, it was not obvious to me that the use is correct. This combination of different disciplines into one model made me comprehend the difference between physical laws and mere tools, a distinction that was vague for me at first, but became clearer as the project progressed.

Furthermore, I went through the process of validating my own numerical results. Sometimes, I felt as if my discretization and simulations are correct, and it is follies in the model that makes the simulations unstable. Other times, when dealing with unpleasant numerical results, I was unsure if my discretization is wrong, or the Python code is wrong. Guided by my advisor, I tried to isolate the problem. The bulk analysis is a result of such a process.

Finally, I would like to thank my advisor, Prof. Yochelis, who pushed me to high standards while directing me in the right direction.

5 Appendix

5.1 Species Synthesis Rate and Flux

The model employs chemical kinetics to describe the rates of biological processes that proteins undergo within the cell's actin cortex. Although chemical kinetics was initially developed for chemical reactions, it finds applications in biological processes as well. As per the law of mass action, a reaction of the form:

$$aA \xrightarrow{k} B \tag{18}$$

has the following rate:

$$\frac{d}{dt}[B] = k[A]^a \tag{19}$$

Here, A and B represent chemical species, $[A]$ and $[B]$ are the concentrations of A and B in molar concentration, and k and a are the reaction rate and stoichiometry constant, respectively. The species flux is described using the transport/continuity equation:

$$\frac{d}{dt}[B] = -\nabla \cdot \mathbf{J} \tag{20}$$

where $\mathbf{J}$ is the species flux in dimensions of $\frac{N}{tL^2}$.

5.2 Discretization of non-homogeneous diffusion

The analytical equations for actin cortex formation involve non homogeneous diffusion and nonlinear boundary conditions. Here, we look at finite difference for non homogeneous diffusion, and how it combines with a regular Neumann boundary condition. The information in this section is primarily derived from [11].

Consider a basic diffusion equation in one dimension with a Neumann boundary condition:

$$\frac{\partial c}{\partial t} = \frac{\partial}{\partial x}\left(D(x)\frac{\partial c}{\partial x}\right) \tag{21}$$

$$\frac{\partial c}{\partial x}\Big|_{x=0} = N(t) \tag{22}$$

Assuming a constant D, we can use forward finite difference for the temporal derivative and central finite difference for the second-order spatial derivative, which is the standard FTCS scheme. If the diffusion is not homogeneous in the solution, then D is a function of space, as we encountered in our model. The difference must account for the changing D as well:

$$c_i^{n+1} = c_i + \frac{\Delta t}{\Delta x^2}\left(D_{i+1/2}(c_{i+1} - c_i) - D_{i-1/2}(c_i - c_{i-1})\right) \tag{23}$$

$$D_{i\pm1/2} \equiv \frac{D_{i\pm1} + D_i}{2} \tag{24}$$

where i and n denote spatial and temporal indices, respectively, and Δt and Δx are the time step and spatial step. From now on, I will omit the superscript n when referring to the current step. Notice that if $D_{i+1/2} = D_{i-1/2}$ then we get the standard FTCS scheme. As for the

boundary, its discretization must match bulk discretization to avoid instability or artificial flux. So for (23), we can use a ghost point c_{-1} for accurate discretization:

$$\frac{c_1 - c_{-1}}{2\Delta x} = N(t) \tag{25}$$

$$c_0^{n+1} = c_0 + \frac{\Delta t}{\Delta x^2}\left(D_{1/2}(c_1 - c_0) - D_{-1/2}(c_0 - c_{-1})\right) \tag{26}$$

$$\Rightarrow c_0^{n+1} = c_0 + \frac{\Delta t}{\Delta x^2}\left[D_{1/2}(c_1 - c_0) - D_{-1/2}\left(c_0 - c_1 + 2\Delta x N(t)\right)\right] \tag{27}$$

5.3 1D Model

The following 1D model is derived from the complete 3D model introduced in subsections 2.1 - 2.2.

$$\frac{\partial p}{\partial t} = -v\frac{\partial p}{\partial x} - \alpha c_b p \tag{28a}$$

$$\frac{\partial m}{\partial t} = \frac{\partial}{\partial x}\cdot(D_m(1-\beta p)\frac{\partial m}{\partial x}) + \alpha c_b p \tag{28b}$$

$$\frac{\partial c_f}{\partial t} = D_c\frac{\partial^2 c_f}{\partial x^2} - k_s c_f p + \alpha c_b p \tag{28c}$$

$$\frac{\partial c_b}{\partial t} = -v\frac{\partial c_b}{\partial x} + k_s c_f p - \alpha c_b p \tag{28d}$$

Where:

$$v = a_{br}k_{br}m^2\big|_{x=0} + k_{gr}(m - m_c)\big|_{x=0} \tag{29}$$

The boundary conditions at $x = 0$ are as follows:

$$\frac{\partial p}{\partial x} = 0 \tag{30a}$$

$$\sum J_{total} = J_m + J_p = D_m(1-\beta p)\frac{\partial m}{\partial x} - vp = 0 \tag{30b}$$

$$\frac{\partial c_f}{\partial x} = 0 \tag{30c}$$

$$c_b = 0 \tag{30d}$$

Boundary conditions at $x = L$:

$$p = 0 \tag{31a}$$

$$\frac{\partial m}{\partial x} = 0 \tag{31b}$$

$$\frac{\partial c_f}{\partial x} = 0 \tag{31c}$$

$$c_b = 0 \tag{31d}$$

6 Bibliography

References

[1] Gat, S. (2022) *Physical Study of a Reconstituted Actomyosin Cortex.* Unpublished doctoral thesis, Department of Chemical Engineering, Ben-Gurion University of the Negev.

[2] Cooper, GM. (2000) *The Cell: A Molecular Approach.* 2nd edition. Sunderland (MA): Sinauer Associates. Structure and Organization of Actin Filaments. Available from: https://www.ncbi.nlm.nih.gov/books/NBK9908/.

[3] Tinevez, J.Y. et al. (2009) *Role of cortical tension in bleb growth.* Proc. Natl. Acad. Sci. U.S.A. 106, 18581–18586.

[4] Salbreux, Guillaume et al. (2012) *Actin cortex mechanics and cellular morphogenesis.* Trends in Cell Biology, 22(10), 536-545. doi:10.1016/j.tcb.2012.07.001.

[5] Manhart, Angelika et al. (2019) *Quantitative regulation of the dynamic steady state of actin networks.* eLife, 8, e42413. doi:10.7554/eLife.42413.

[6] Carlsson, A.E. et al. (2004) *End versus side branching by Arp2/3 complex.* Biophysical Journal, 86(2), 1074-1081. doi:10.1016/S0006-3495(04)74182-X.

[7] Cengel, Y.A. and Cimbala, J.M. (2014) *7 - Dimensional Analysis and Modeling.* In: Fluid Mechanics: Fundamentals and Applications. New York: McGraw-Hill.

[8] Manhart, A. et al. (2019) *Quantitative regulation of the dynamic steady state of actin networks.* eLife, 8. doi:10.7554/elife.42413.

[9] Michalski, P.J. and Carlsson, A.E. (2010) *The effects of filament aging and annealing on a model lamellipodium undergoing disassembly by severing.* Physical Biology, 7(2), 026004. doi:10.1088/1478-3975/7/2/026004.

[10] Rouiller, I. et al. (2008) *The structural basis of actin filament branching by the Arp2/3 complex.* J Cell Biol, 180(5), 887-895. doi:10.1083/jcb.200709092.

[11] Press, W.H. and Vetterling, W.T. (2007) *Chapter 20.* In: Numerical Recipes. Cambridge: Cambridge University Press.